JOURNAL OF MATERIALS SCIENCE 31 (1996) 3487–3495

The formation of hollow spherical ceramic oxide particles in a d.c. plasma

G. PRAVDIC, M. S. J. GANI
Department of Materials Engineering, Monash University, Clayton, Victoria 3168, Australia

Investigations have been carried out to determine the conditions that lead to the production of spherical hollow ceramic oxide particles during melting in a d.c. plasma jet. Reports in the literature indicated that such ceramic particles were formed by plasma spraying spray dried agglomerates, but precise details of the conditions necessary for their formation were not stated. In this study it is shown that for hollow particles to be formed several conditions had to be met. Spherical spray dried agglomerates had to be used as starting materials, the material being sprayed had to melt over a narrow temperature range and the size of the particles had to exceed a certain diameter. Experiments, using yttria, showed that the relative size of the pore was dependent on particle diameter, and it has been proposed that the major controlling factor that influences this dependence is the escape of gas trapped in the spray dried agglomerate during melting rather than surface tension or undercooling which were shown to produce only minor effects. In addition, the results also showed that the nature of porosity within the hollow particles as well as the surface morphology was dependent on the material being sprayed.

1. Introduction

Plasma spraying of ceramic powders is normally used to produce ceramic coatings on metallic substrates for the improvement of wear properties or to act as thermal barriers. In the many investigations that have been carried out into the production of ceramic coatings by this method there have been some reports of the production of hollow particles during the plasma melting of powders which led to increased porosity in the sprayed coatings. In some cases this was used to produce controlled porosity in coatings on turbine engine blades, diesel engines or as abradable coatings [1–3]. By incorporating porosity into the coating, the thermal insulation and mechanical toughness of the coating can also be enhanced [2]. It was noted that many of these hollow ceramic particles resulted from the plasma spraying of spray dried powders, but precise details of the conditions necessary for their formation were not given [3–5].

2. Experimental procedure

The source, chemical composition, morphology and approximate particle size of the ceramic powders used in this study are shown in Table I.

With the exception of ZrO_2/Y_2O_3 which was supplied as a commercially prepared spray dried powder, all the other materials were wet attrition milled (where necessary) to reduce the particle size to $< 1\ \mu m$, and then the aqueous suspensions were spray dried using a Niro rotary atomizer Denmark. Most of the suspensions used for spray drying were prepared by ultrasonically dispersing the powder in distilled water. However, in some cases, acetic acid or ammonia additions were made to control the viscosity of the suspension or up to 8 wt % polyvinyl alcohol (PVA) was added to act as a binder for the spray dried agglomerates. Some spray dried agglomerates that did not contain a binder had to be partially sintered prior to plasma spraying in order to prevent their disintegration in the plasma torch feed lines which resulted in blockage of the lines.

A subsonic (atmospheric) d.c., plasma torch (Plasmadyne SG–100, 40 kW, 900 A) with Ar ($44\ l\ min^{-1}$) and He ($4\ l\ min^{-1}$) plasma gases, equipped with a Metco powder feed unit type 4MP model 851 was used to plasma spray the powders which were collected in distilled water.

The surface morphology and internal structure of both the spray dried and plasma sprayed particles were determined using a scanning electron microscope, Jeol SEM (JSM 840A). The internal structure of the particles was observed by either sectioning particles set in an epoxy resin or by the examination of the shells of crushed particles. Quantitative measurements to determine the size of the pore within yttria particles and the particle diameters were obtained from optical micrographs of the particles dispersed in methylene iodide which were taken using an Olympus BHSP microscope under plane polarized transmitted light. A pycnometer was used to measure the density of yttria powders which had been sized by sieving.

3. Results

3.1. Spray dried powders

For the production of spherical spray dried agglomerates there was an optimum solids content in the slurry,

TABLE I The materials and their source, composition, particle morphology and approximate particle size used in the investigations.

Material	Source	Composition	Morphology and approximate particle size
Y_2O_3	Aldrich Chemical Co. Ltd.	Y_2O_3	Angular particles, approx. size range between 5–10 μm.
ZrO_2–Y_2O_3 (SY Ultra 5.2)	Z-Tech, ICI Advanced Ceramics	ZrO_2 + 5.1 wt % Y_2O_3	Spherical spray dried agglomerates consisting of particles < 1 μm. The mean agglomerate size was between 5–100 μm.
Talc (TX) $3MgO.4SiO_2.H_2O$	Steetley Minerals	SiO_2 + 33.5 wt % MgO	Platelets, 20–30 μm in length and 5–10 μm thick.
Al_2O_3	Linde, High Purity Abrasive, ex Union Carbide	Al_2O_3	Angular particles, approx. size range between 5–30 μm
Al_2O_3/TiO_2	Rf plasma prepared powder in Materials Engineering, Monash University	Al_2O_3 + 34.2 wt % TiO_2	Spherical, solid particles. Mean particle size 0.1 μm
TiO_2	Ajax Chemicals	TiO_2	Angular particles less than 1 μm.

the value of which was dependent on the nature of the material being sprayed. Concentrations of slurries below this optimum resulted in the production of doughnut shaped agglomerates, which were found not to produce hollow particles after plasma spraying, and higher concentrations resulted in the blocking of the atomizer of the spray drier.

3.2. Internal structure of plasma sprayed powders

All of the plasma sprayed particles except the TiO_2/Al_2O_3 particles, exhibited porosity but the distribution and amount of porosity differed as shown in Figs 1–7.

As shown in the SEM micrographs (Figs 1 and 2) the majority of the larger ZrO_2/Y_2O_3 and Y_2O_3 particles each contained a single smooth lined spherical pore, however in some of the ZrO_2/Y_2O_3 particles (Fig. 3) the interior of the shells was rough. MgO/SiO_2 contained numerous small pores within each particle (Fig. 4). Al_2O_3 and TiO_2 contained some remnant material within the cavity which often was present as a small spherical particle trapped within the outer shell, as shown in Figs 5 and 6. Although there were a few hollow Al_2O_3/TiO_2 particles produced, the majority of the particles were observed to be solid (Fig. 7).

3.3. Measurements of pore size as a function of particle size for yttria particles

The dependence of the pore size on particle size was determined from measurements of photographs of images of particles in optical micrographs of plasma sprayed yttria particles. A typical micrograph is shown in Fig. 8. The results obtained by these quantitative measurements of the internal pore size and the external particle size which were converted to the ratio of the pore volume to particles volume and plotted against particle size are shown in Fig. 9. Density data determined on powders sieved into various size ranges also indicated a dependence of pore size on particle size in that the measured density decreased as the particle size increased. These results are shown in Table II.

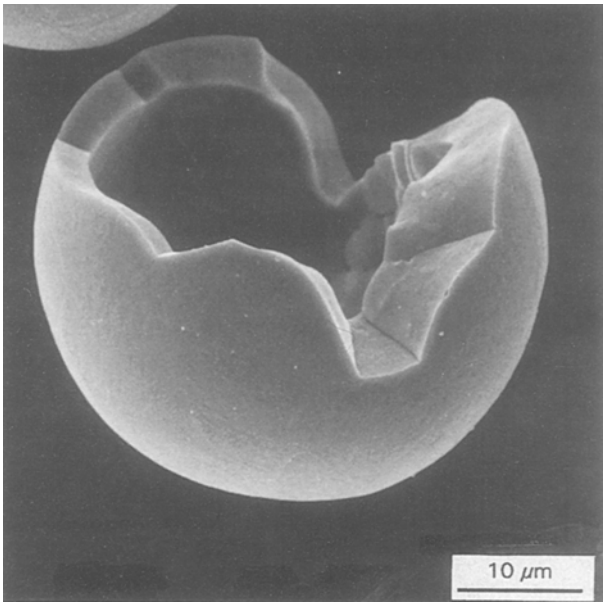

Figure 1 A ZrO_2/Y_2O_3 broken particle.

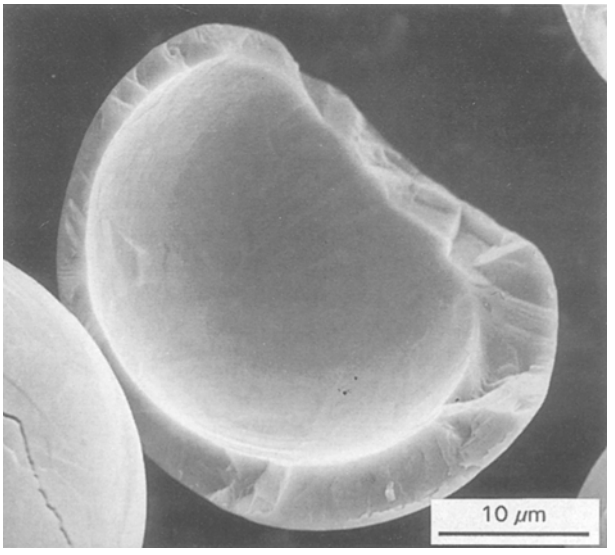

Figure 2 A Y_2O_3 broken particle.

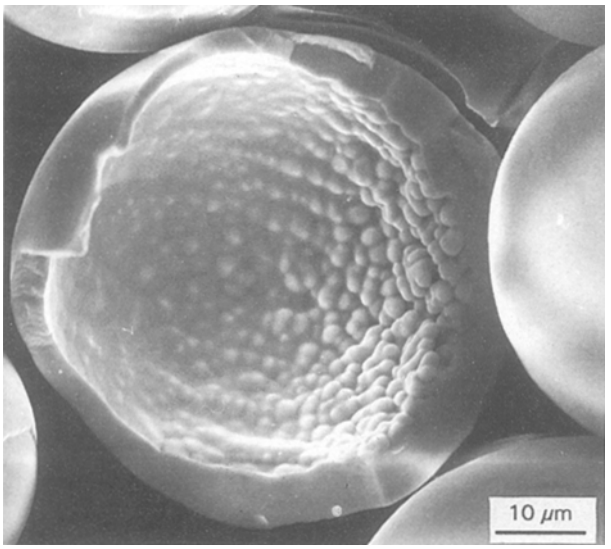

Figure 3 A ZrO_2/Y_2O_3 particle showing a rough interior surface.

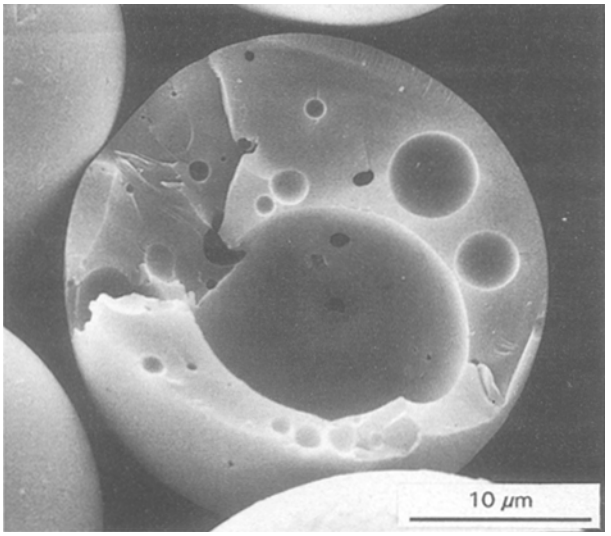

Figure 4 A MgO/SiO_2 broken particle.

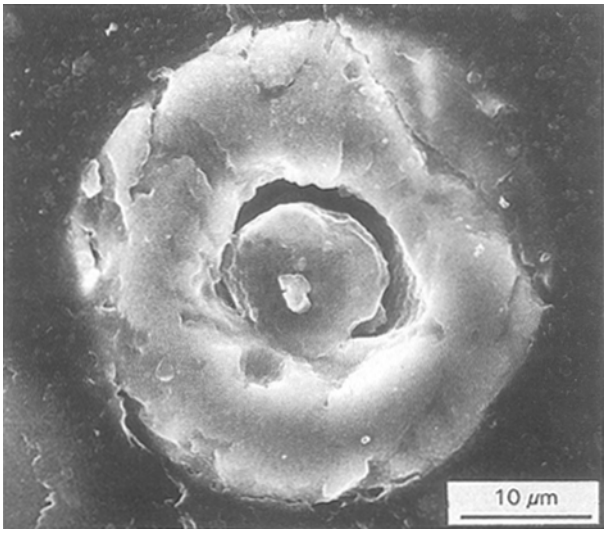

Figure 5 Cross-section of an Al_2O_3 particle.

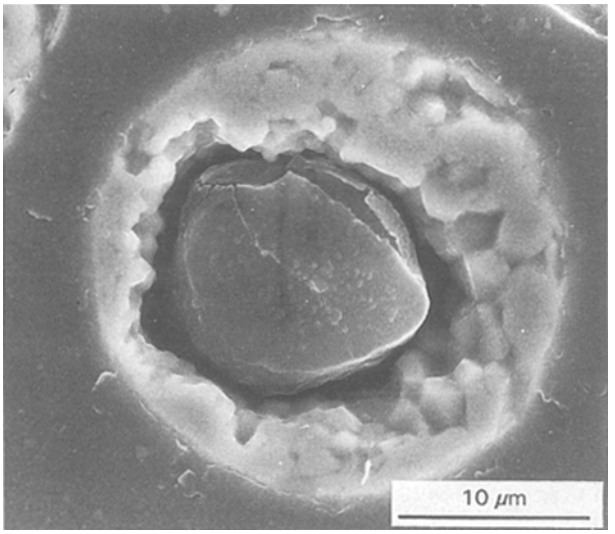

Figure 6 Cross-section of a TiO_2 particle.

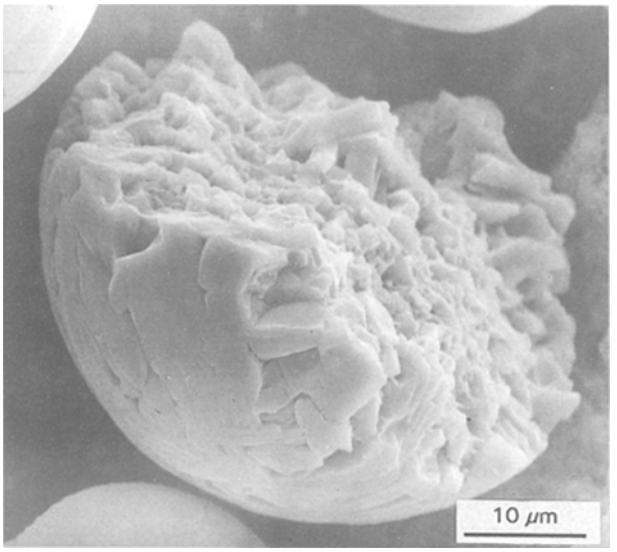

Figure 7 Broken particle of Al_2O_3/TiO_2.

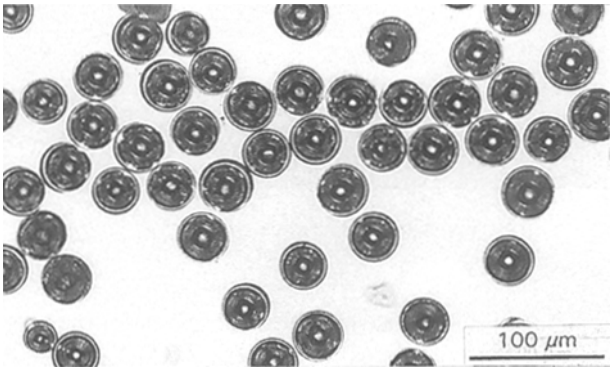

Figure 8 Optical micrograph of yttria particles (size range 38–45 μm).

3.4. Surface morphology of the plasma sprayed powders

The surface of the plasma sprayed particles showed distinctly different morphologies for each of the materials illustrated by SEM micrographs in Figs 10–15.

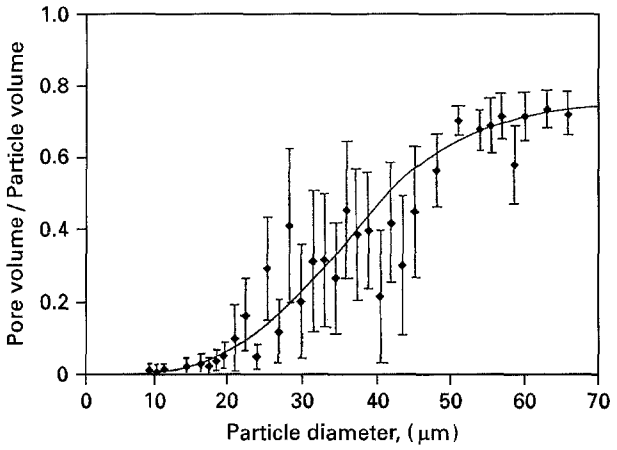

Figure 9 Ratio of internal pore volume to particle volume as a function of particle size.

TABLE II Measured density of sieved yttria powders.

Particle size range (μm)	Measured density (kg m^{-3})
< 20	4.74 ± 0.04
20–38	4.35 ± 0.04
38–45	3.40 ± 0.04
45–53	2.77 ± 0.04
53–71	2.50 ± 0.04

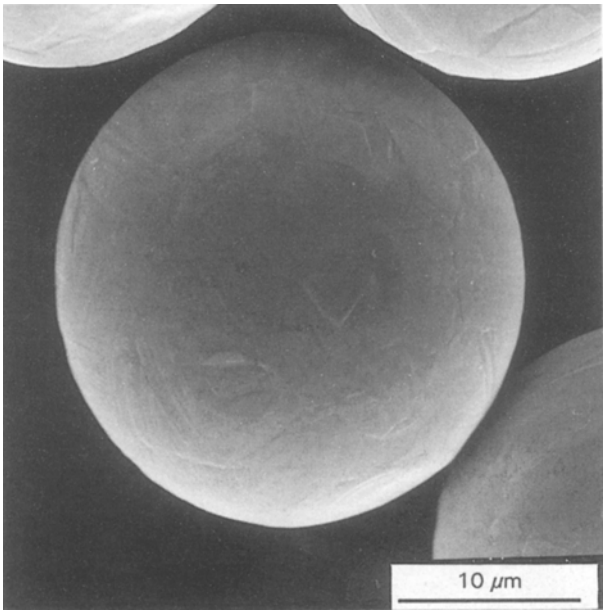

Figure 10 Surface of an Y_2O_3 particle.

Smooth exterior surfaces were observed for the fully spheroidized particles of Y_2O_3, ZrO_2/Y_2O_3 and MgO/SiO_2 (Figs 10–12). However closer examination of yttria particles revealed that some of the apparently smooth surfaces actually consisted of roughly hexagonal shaped grains or parallel lines. Fine dendritic crystals could be seen on the surface of the Al_2O_3 particles (Fig. 13) whereas for the Al_2O_3/TiO_2 particles shown in Fig. 14, the surface consisted of larger grains containing dendritic crystals. The surface morphology of the TiO_2 particles (Fig. 15) contained large roughly hexagonal shaped grains.

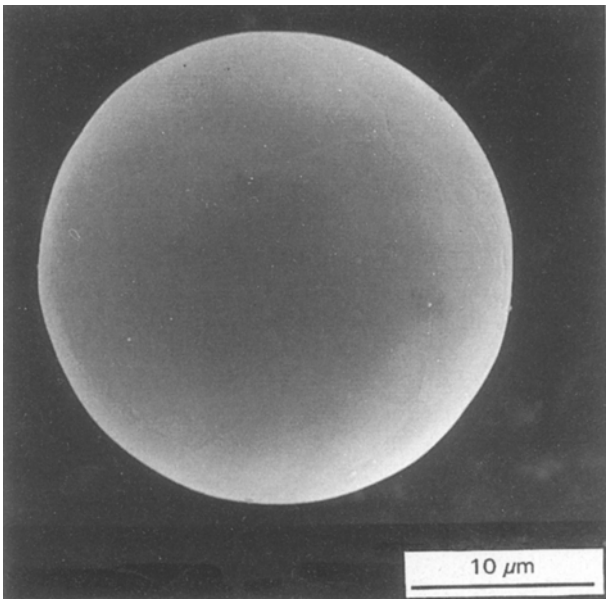

Figure 11 Surface of ZrO_2/Y_2O_3 particle.

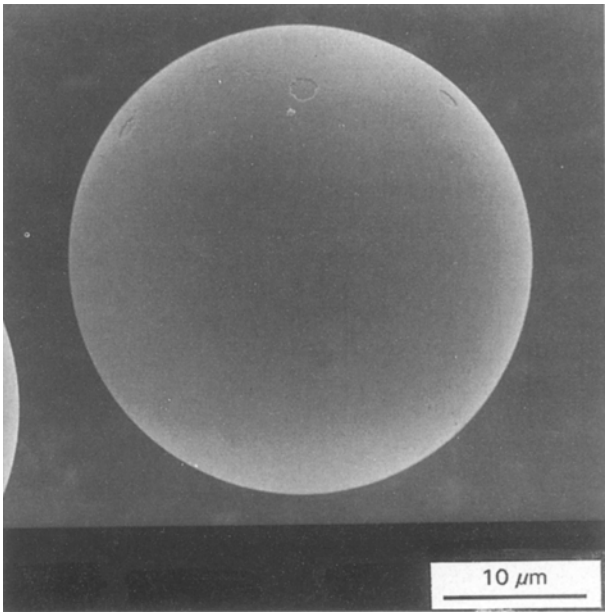

Figure 12 Surface of MgO/SiO_2 particle.

4. Discussion

4.1. The relationship between pore size and particle size in yttria powders

The detailed investigation carried out on plasma sprayed yttria particles showed that there was a dependence of pore size on particle size as shown in Fig. 9. Particles less than 10 μm diameter contained little or no porosity whereas the ratio of the pore volume to particle volume increased with increasing particle diameter for particles with diameters between 10–60 μm. The larger sized particles tended towards a constant pore volume/particle volume ratio of 0.7.

The densities of particles for various size ranges corresponding to those obtained by sieving were calculated from the optical data and compared with the densities measured using the pycnometer. The results

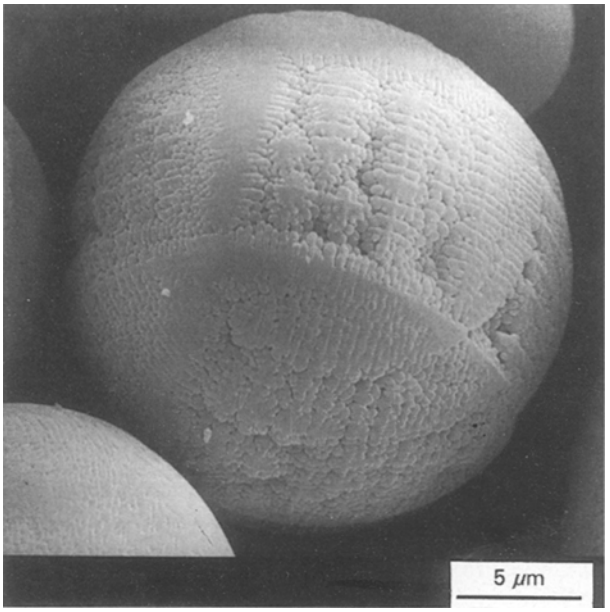

Figure 13 Dendrites on the surface of Al_2O_3 particle.

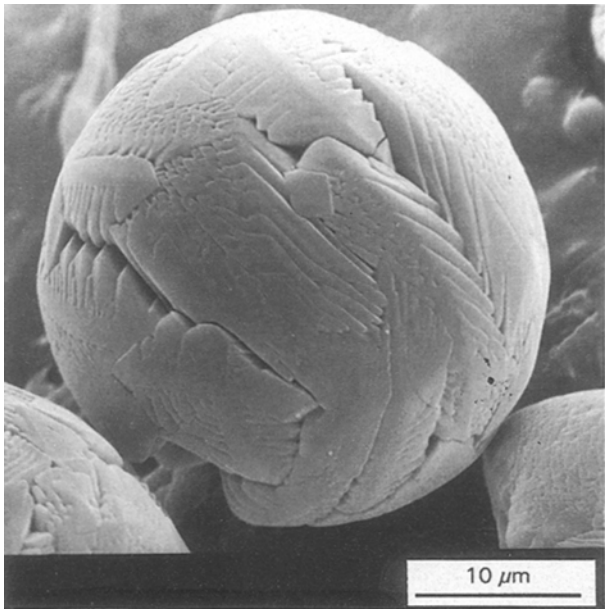

Figure 14 Surface morphology of Al_2O_3/TiO_2 particle.

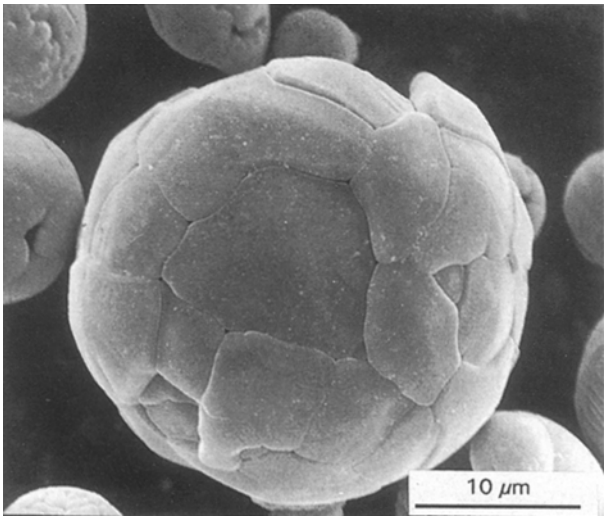

Figure 15 Surface morphology of TiO_2 particle.

TABLE III Comparison of measured density of sieved yttria powders with the density calculated from data presented in Fig. 17.

Particle size range (μm)	Measured density (kg m^{-3})	Calculated density (kg m^{-3})
< 20	4.74 ± 0.04	4.7_8–5.0_3*
20–38	4.35 ± 0.04	2.9_2–4.7_8
38–45	3.40 ± 0.04	2.5_9–2.9_2
45–53	2.77 ± 0.04	1.7_1–2.5_9
53–71	2.50 ± 0.04	1.3_1–1.7_1

* Theoretical density of yttria = 5.03 kg m^{-3}.

are shown in Table III. The measured density shows similar trends to that calculated from optical measurements, in that the densities decreased with increasing particle size, but the value of the measured densities were higher. This could be attributed to the presence of broken particles in the sieved material which would have the effect of increasing the overall density of the powder.

In order to investigate the factors that could influence the observed dependence of pore size within particles, calculations of the pore size as a function of particle size were carried out. The following assumptions were made in the calculations:

(a) The total volume of solid particles in the spray dried agglomerate was 60%. (If the solid particles in the agglomerate were all spherical, of uniform size and close packed, then this value would be 74 vol %. Random packing would be expected to reduce the density of packing.)

(b) That as the spray dried agglomerate melts in the plasma, gas in the outer layer of the agglomerate escapes, whereas gas in the centre of the agglomerate is trapped within the molten shell. The thickness of this outer layer can be estimated from the observation that 10 μm diameter particles contained little or no porosity which would indicate that gas could escape through a 5 μm layer during the melting of the agglomerate.

(c) The trapped gas is heated and expands (ideal gas behaviour has been assumed).

(d) The final volume of trapped gas is determined by the temperature at which the liquid yttria freezes (T_f).

Initial calculations were carried out to determine whether the assumption of the formation of a liquid outer layer which prevented further escape of gas from the agglomerate was reasonable. The results are presented graphically in Fig. 16 (experimentally measured data points are included for comparison). Three thickness values were used in calculations, 5, 7.5 and 10 μm. The results of these calculations and the measured data points show that the calculated curves have a similar shape to the measured dependence of pore volume on particle volume. The closest match to the experimental results is obtained with a 7.5 μm layer.

This strong dependency of pore size on the thickness of the layer through which the gas can escape during melting gives an explanation of why it was found essential to use spherical spray dried agglomer-

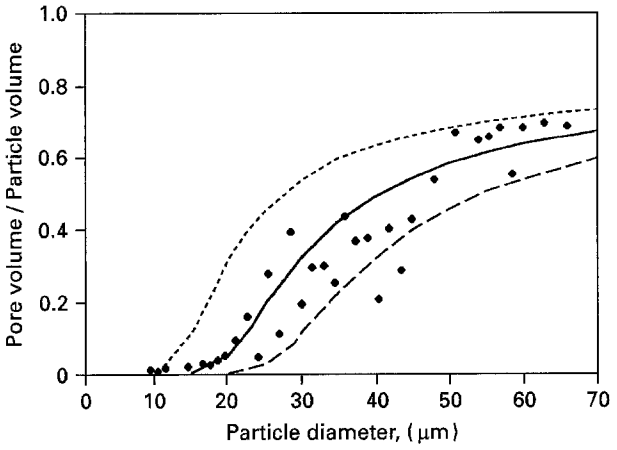

Figure 16 Calculated pore volume/particle volume as a function of particle size. The experimental points are represented by the symbol (◆). The calculated fits to this data were attempted using; (- - -) a 5 μm layer, (—) a 7.5 μm layer and (– –) a 10 μm layer.

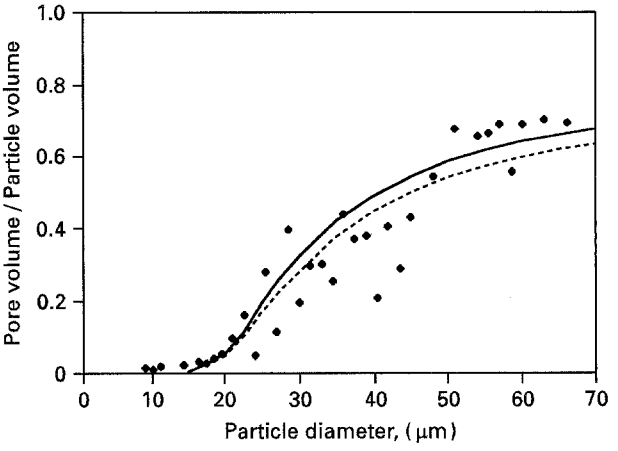

Figure 18 The effect of the freezing temperature of the liquid droplets on pore size. The measured points are represented by the symbol (◆). The data was fitted assuming a 7.5 μm layer with the conditions; (–) no undercooling and (- - -) undercooling to 2216.5 K.

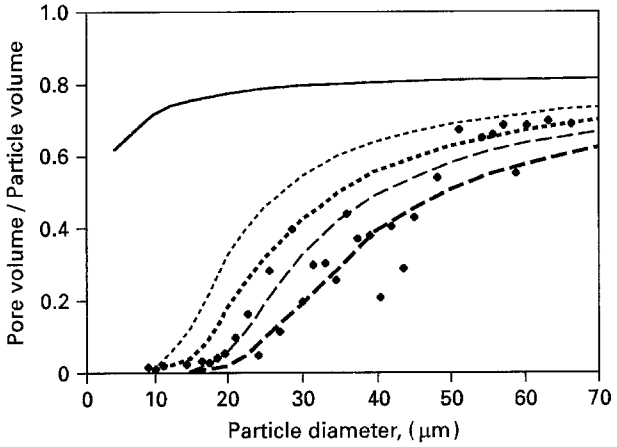

Figure 17 The effect of surface tension. The measured points are represented by the symbol (◆). The data fits were attempted using the following conditions; (—) only surface tension (500 mJ m^{-2}), (- - - -) layer thickness = 5 μm, surface tension = 0, (▬) layer thickness = 5 μm, surface tension = 500 mJ m^{-2}, (– –) layer thickness = 7.5 μm, surface tension = 0 and (▬▬) layer thickness = 7.5 μm, surface tension = 500 mJ m^{-2}.

ates in order to produce hollow particles. The 'doughnut' shaped agglomerates that were produced if the slurry used in spray drying was too dilute did not produce many hollow particles when plasma sprayed, presumably because of the larger surface area/volume ratio of these particles permitted the escape of gas in the agglomerate during melting and thus resulted in the production of mainly solid particles.

The above calculations do not take into account the possible effects of surface tension of the liquid droplets on the volume of the gas trapped within the particle. If this is taken into account then the resulting values are as shown in Fig. 17. Unfortunately no experimentally measured values of the surface tension of liquid yttria could be found. The value of 500 mJm^{-2} for surface tension used in the calculation was selected so as to be similar to that of other molten oxides namely TiO_2 (380 mJm^{-2}) [6], ZrO_2 (435 mJm^{-2}) and Al_2O_3 (665 mJm^{-2}) [7].

Fauchais *et al.* [5] used the increase of pressure within a hollow liquid droplet, brought about by surface tension effects as the particle diameter is decreased, to explain why small ZrO_2/8 wt % Y_2O_3 particles less than 40 μm were solid, whereas the larger particles contained pores. The calculated values for the effect of surface tension on the pore volume/particle volume ratio in the particle size range 5–70 μm demonstrates that surface tension effects cannot solely be used to explain the observed dependency of pore size on particle size in the system under study, as is shown in Fig. 17. However, if surface tension is included in the calculations using the thickness of the outer layer through which gas can escape during the melting of the spray dried agglomerates, then it can be seen in Fig. 17 that a layer thickness of between 5–7.5 μm produces reasonable agreement with observations.

The above calculations have also been made with the assumption that the liquid droplet freezes at the equilibrium freezing point of yttria (T_f = 2703 K). However when isolated liquid droplets are rapidly cooled a large degree of undercooling is expected to take place. This undercooling was calculated by McPherson [8] to be 0.82 T_f, which would correspond to a temperature of 2216.5 K for yttria. The effect of this undercooling on the pore size is shown in Fig. 18 which shows that the lowering of the solidification temperature from the equilibrium freezing point of the liquid droplets to 2216.5 K only leads to a small reduction in the pore size as a function of particle size.

Other factors that could possibly have minor effects on the pore volume include the evolution of adsorbed gas present on the surface of the particles in the agglomerate, the burnout of the PVA binder (when used) and possible evaporation of Y_2O_3 (which has been reported previously by Gitzhofer *et al.* [9]). All of these would be expected to result in a small increase in the volume of the pore within the particle.

The above calculations show that the major factor that influences the dependency of pore size on the particle size is that of the thickness of the layer through which the gas in the agglomerate can escape during the melting of the agglomerate. If this assumption

is correct, it would be expected that the thickness of this layer would also be strongly dependent on the temperature range over which melting takes place. A large melting range would increase the time available for gas to escape and therefore result in an increase of the thickness of the layer. This hypothesis is supported by observations in the other systems studied. The single component systems, alumina and titania, have sharp melting points and therefore would be expected to form an enclosed pore, as was observed to be the case. Examination of the phase diagrams of the two component systems (ZrO_2/5.1 wt % Y_2O_3 [10], MgO/66.5 wt % SiO_2 [11] and Al_2O_3/34.2 wt % TiO_2 [12]) shows that both the ZrO_2–Y_2O_3 and MgO–SiO_2 agglomerates would be expected to melt over a narrow temperature range of about 5 °C, whereas the Al_2O_3–TiO_2 agglomerates have a melting range of up to 175 °C. This wide melting range, from the eutectic to the melting point of pure alumina, is a result of the variation in composition of the individual plasma prepared submicrometre particles that made up the agglomerates. Most of the plasma sprayed Al_2O_3–TiO_2 particles were observed to be solid, which is consistent with the large melting range of the agglomerates whereas the plasma sprayed ZrO_2–Y_2O_3 and MgO–SiO_2 agglomerates which melted over narrow temperature ranges formed hollow particles. Huang and Ding [13] observed that a plasma sprayed spray dried Al_2O_3–TiO_2 powder (of unknown composition) also resulted in the production of solid particles.

As already shown, all of the plasma sprayed particles except the TiO_2/Al_2O_3 particles contained pores, however the distribution and size of the pores differed. Y_2O_3 particles contained a single void (providing the diameter of the particles was greater than 10 μm). A single isolated void was also observed in ZrO_2/Y_2O_3 particles. Numerous closed pores were observed within the MgO/SiO_2 particles which could be due to the high viscosity of the silicate melt which would make it difficult for the trapped pores to coalesce to form a single void. The plasma sprayed Al_2O_3 and TiO_2 particles contained some material within the hollow cavity which was often present as a small spherical particle trapped within the outer shell. The formation of the enclosed particle could be due to the thermal properties of the liquid oxides. For example, low thermal conductivity and low emissivity of the liquids would tend to hamper heat transfer from the particle surface to the centre of the particles during the short residence time in the plasma and result in the presence of some unmelted, or partially melted material, usually in the form of a smaller particle in the centre of the hollow cavity of the outer particle.

4.2. Surface morphology of plasma sprayed powders

When spray dried agglomerates of ZrO_2/5.1 wt % Y_2O_3 were plasma sprayed, the surface morphology of the resultant fully spheroidized particles (10–70 μm) was observed to be smooth. SEM micrographs of a plasma sprayed ZrO_2/8 wt % Y_2O_3 sol–gel prepared powder also showed particles (10–50 μm) with smooth surfaces, but no explanation for the smooth surface was given by the authors [14]. However, fine dendritic grains were present on the surfaces of pure zirconia particles (75 μm diameter) which had been prepared by passing comminuted non-spherical particles through an extended arc [15]. It was proposed that the formation of dendrites was promoted by the rapid cooling rate experienced by these particles emerging from the high temperature source. 'Microballoons' of ZrO_2, prepared by Gilman [16] using an inductively coupled plasma torch (50% Ar–50% N_2 plasma gases) also had a textured surface and, according to the author, this was indicative of a strained surface.

In this investigation, plasma sprayed Y_2O_3 particles were also observed to have an apparently smooth surface, however when the particles were more closely examined, the surfaces of some of the particles contained some roughly hexagonal shaped grains or in some cases parallel lines. Bildstein [17] and McPherson [18] who have also prepared plasma sprayed Y_2O_3 particles, made no comment on the surface texture of the particles.

When talc ($3MgO.4SiO_2.H_2O$) was plasma sprayed, the resultant particles (MgO/SiO_2) again exhibited smooth surfaces. No reports from the literature have been found of plasma spraying MgO/SiO_2 particles, however studies undertaken on individual MgO (100 μm) and SiO_2 (75 μm) microspheres prepared in an extended arc by Pickles and McLean [15] also showed the surfaces of these particles to be smooth and featureless.

Plasma sprayed Al_2O_3 powders had fine dendritic crystals on the surfaces of the particles. Dendritic crystals have been reported in previous studies for plasma sprayed alumina powders by Waldie [19], Lyagushkin and Solonenko [20] and Nelson *et al.* [21]. Waldie who prepared the powders by introducing irregular shaped alumina particles into radio-frequency (r.f.) argon plasma, found that the dendritic patterns were not observed on all of the alumina particles. He suggested that this could be due to different temperature histories experienced by the particles within the plasma. This could have been due to steep radial temperature gradients created in the r.f. plasma due to non-uniform gas velocities and/or differences in the size and shape of the particles introduced into the induction plasma. Nelson *et al.* [21], melted drops of alumina (approximate size 3 mm) using a carbon dioxide laser in an argon and oxygen atmosphere. They found that by melting drops of alumina in an argon atmosphere, dendritic growth was observed on the surfaces of the resultant particles accompanied by the formation of a single centro-symmetric void. Those particles produced using an oxygen atmosphere, resulted in the formation of trigonally arranged lamellae throughout the bulk of the drops. The particles were also found to be more porous and rougher as compared to those produced in an argon atmosphere. These results showed that the atmosphere has an effect on the surface morphology of the resultant alumina particles. The use of an oxygen-deficient atmosphere

such as argon, produced dendritic grains on the surface of the alumina particles. Similarly dendritic grains were obtained in the present study when alumina was plasma sprayed in an argon–helium plasma.

When spray dried agglomerates of Al_2O_3/TiO_2 were plasma sprayed, the surface of the resultant particles also exhibited dendritic grains whilst for the plasma sprayed TiO_2 particles, large roughly hexagonal shaped grains were observed on the surface of the particles. No reports have been found which describe the surface morphology of particles of either Al_2O_3/TiO_2 or TiO_2.

5. Conclusions

Experiments have been undertaken in this study to determine the important parameters that lead to the production of spherical hollow ceramic oxide particles, with diameters from 5–80 μm, using a d.c. plasma jet.

Detailed experimental measurements were undertaken using the yttria system and the results showed that there was a dependence of the relative pore size as a function of particle size. These results were then compared with those obtained from calculated pore size as a function of the particle size. The calculated results showed that the major factor that influences the dependency of the pore size as a function of the particle size was the effect of the thickness of the outer layer through which the gas in the spray dried agglomerate could escape during the melting of the agglomerate before an impervious liquid skin could be formed entrapping any remaining gas within the rest of the agglomerate and thus forming a void. It was found that if the gas was assumed to escape in the outer 7.5 μm layer of the agglomerate, the calculated curve was found to lie close to that of the measured curve. When surface tension or undercooling effects were included in the calculations, these were shown to produce only a minor effect on the relative size of the pore within the particle.

If the thickness of the layer through which the gas can escape is assumed to be the major parameter that effects the size of the pore within the particle this would explain why it was necessary to prepare spherical spray dried agglomerates in order to produce hollow particles. When 'doughnut' shaped agglomerates were plasma sprayed, the majority of the resultant particles were observed to be solid. The possible reason for this could be due to more gas escaping from the porous agglomerate during the melting process because the surface area/volume ratio of these agglomerates would be higher.

It was also found that the temperature range over which melting of the agglomerate occurs could be another controlling parameter for the formation of hollow particles. The observation that the majority of the Al_2O_3–TiO_2 particles were solid could be attributed to the large temperature range over which melting occurred and thus allowing more gas to escape. Whereas by plasma spraying agglomerates made from materials that either melted over a narrow temperature range such as the Y_2O_3–ZrO_2 and MgO/SiO_2 systems or have a sharp melting point such as the Y_2O_3, Al_2O_3 and TiO_2 systems, the resultant plasma sprayed powders all exhibited porosity but the distribution and amount of porosity differed for each material.

The effect of the pore size as a function of the particle size was also undertaken by measuring the density of the plasma sprayed yttria powders that were sieved into different size ranges and then compared with calculated density measurements as determined from the pore of the particles obtained from optical micrographs. The results showed that the measured density was significantly greater than that obtained from the calculated density measurements. This could be due to the presence of non porous fines and broken particles which would increase the measured density of the powder.

The internal structure of the hollow particles were also found to be dependent on the material system. Some of the important material properties which could have an effect on the type of porosity produced within the particle include the effect of viscosity of the molten material and the effect of heat transfer through the agglomerate.

The surface morphology of the plasma sprayed particles was also found to be dependent on the material system used. Studies undertaken by other researchers indicated that the surface morphology of the plasma sprayed particles could also be dependent on other factors such as the type of atmosphere used in which the particles were prepared, the temperature history experienced by the particles within the high heat source and also the size or shape of the particles introduced into the high heat source.

References

1. M. F. GRUNINGER and M. V. BORIS, in Proceedings of the International Thermal Spray Conference, Orlando, Florida, U.S.A., 28 May to 5 June 1992, edited by C. C. Berndt (ASM International, Materials Park, Ohio, 1992) p. 487.
2. H. HERMAN, C. C. BERNDT and H. WANG, "Ceramic Films and Coatings", edited by J. B. Wachtman and R. A. Haber (Noyes Publications, Park Ridge, NJ, 1993) p. 148.
3. F. N. LONGO, N. F. BADER and M. R. DORFMAN, Eur. Pat. Appl. EP 86,938 (Cl c23D5/10) (1983).
4. D. B. OTT and B. A. KUSHNER, in Proceedings of the Third National Thermal Conference, Long Beach, California, U.S.A., 20-25 May 1990, edited by T.F. Bernecki (ASM International, Materials Park, Ohio, 1991) p. 93.
5. P. FAUCHAIS, M. VARDELLE, A. VARDELLE and J. F. COUDERT, *Metall. Trans. B.* **20B** (1989) 263.
6. V. I. KOSTIKOV, V. YA. LEVIN, M. A. MAURAKH and B.S. MITIN, *Sb. Mosk. Inst. Stali. Splavov* **49** (1969) 125.
7. J. M. LIHRMANN and J. S. HAGGERTY, *J. Amer. Ceram. Soc.* **68** (1985) 81.
8. R. McPHERSON, *J. Mater. Sci.* **8** (1973) 851.
9. F. GITZHOFER, A. VARDELLE, M. VARDELLE and P. FAUCHAIS, *Mater. Sci. and Engng.* **A147** (1991) 107.
10. R. S. ROTH, T. NEGAS and L. P. COOK, in "Phase Diagrams for Ceramists", Vol. IV., edited by G. Smith (The American Ceramic Society, Columbus Ohio 1981) p. 141.
11. W. D. KINGERY, H. K. BOWEN and D. R. UHLMANN, in "Introduction to Ceramics" Second Edition (John Wiley and Sons, New York, 1976) p. 288.
12. E. M. LEVIN, C. R. ROBBINS and H. F. McMURDIE, in "Phase Diagrams for Ceramists", edited by M. K. Reser (The American Ceramic Society, Columbus, Ohio, 1964) p. 123.

13. B. HUANG and C. DING, in Proceedings of International Symposium on Advanced Thermal Spraying Technology and Allied Coatings '88, Osaka, Japan, May 1988, (High Temperature Society of Japan, Osaka, 1988) p. 185.
14. M. A. HEDGES and R. TAYLOR, in Proceedings of the Third National Thermal Spray Conference, Long Beach, California, U.S.A., 20–25 May 1990, edited by T. F. Bernecki (ASM International, Materials Park, Ohio, 1991) p. 59.
15. C. A. PICKLES and A. McLEAN, *Ceram. Bull.* **62** (1983) 1004.
16. W. S. GILMAN, *ibid.* **46** (1967) 593.
17. H. BILDSTEIN, *Chem.-Ingr.-Techn.* **38** (1966) 19.
18. R. McPHERSON, *J. Mater. Sci.* **18** (1983) 1341.
19. B. WALDIE, *J. Mater. Sci. Lett.* **4** (1969) 648.
20. V. P. LYAGUSHKIN, O. P. SOLONENKO, P. Y. PEKSHEV and V. A. SAFIULLIN, in Proceedings of 8th International Symposium of Plasma Chemistry (ISPC–8) edited by K. Akashi and A. Kinbara (Univ. of Tokyo, Tokyo, 1987) p. 1964.
21. L. S. NELSON, N. L. RICHARDSON, K. KEIL and S. R. SKAGGS, *High Temp. Sci.* **5** (1973) 138.

Received 9 May 1995
and accepted 1 December 1995